Current Oncology Reports (2023) 25:1213–1226
https://doi.org/10.1007/s11912-023-01452-y

New Developments in Image-Guided Percutaneous Irreversible Electroporation of Solid Tumors

Jung H. Yun[1] · Adam Fang[2] · Fereshteh Khorshidi[2] · Peiman Habibollahi[3] · Oleksandra Kutsenko[4] · Vahid Etezadi[2] · Stephen Hunt[5] · Nariman Nezami[2,6]

Accepted: 21 August 2023 / Published online: 11 September 2023

Abstract

Purpose of Review This review will describe the various applications, benefits, risks, and approaches of conventional irreversible electroporation (IRE), as well as highlight the new technological developments of this procedure along with their clinical applications.

Recent Findings Minimally invasive image-guided percutaneous IRE ablation has emerged as a newer, non-thermal ablation technique for tumors in the solid organs, particularly within the liver, pancreas, kidney, and prostate. IRE allows for ablation near heat-sensitive structures, including major blood vessels and nerves, and is not susceptible to the heat sink effect. However, it is limited by certain requirements, such as the need for precise parallel placement of at least two probes with a maximum inter-probe distance of 2.5 cm to reduce the risk of arching phenomenon, the requirement for general anesthesia with muscle relaxant, and the need for cardiac synchronization. However, new technological advancements in the ablation system and image guidance tools have been introduced to improve the efficiency and efficacy of IRE.

Summary IRE is a safe and effective treatment option for solid tumor ablation within the liver, pancreas, kidney, and prostate. Compared with other ablation techniques, IRE has several advantages, such as the absence of heat sink effect and minimal injury to blood vessels and bile ducts while activating the immune system. Novel techniques such as H-FIRE, needle placement systems, and robotics have enhanced the accuracy and performance in placement of IRE probes. IRE can be especially beneficial when combined with chemotherapy, immunomodulation, and immunotherapy.

Keywords Percutaneous · Ablation · Irreversible electroporation · Pulse electric field · Tumor

Introduction

Minimally invasive image-guided tumor ablation techniques have been established as safe, efficient methods to treat tumors, particularly those that are surgically unresectable. The four most common types of tumor ablation include radiofrequency ablation (RFA), microwave ablation (MWA), cryoablation, and percutaneous ethanol ablation. RFA and MWA are the most frequently used ablation methods but are limited by the tumor location and presence of nearby heat-sensitive structures. RFA is particularly susceptible to the heat-sink effect in which blood flow near the ablation zone causes loss of heat secondary to convection and results in incomplete ablation [1, 2]. Irreversible electroporation (IRE) has emerged as a newer, non-thermal ablation technique for the treatment of solid organ tumors including liver, pancreas, kidney, and prostate.

✉ Nariman Nezami
dr.nezami@gmail.com

1 Division of Vascular and Interventional Radiology, Jefferson Einstein Hospital, Philadelphia, PA, USA

2 Division of Vascular and Interventional Radiology, Department of Diagnostic Radiology and Nuclear Medicine, University of Maryland School of Medicine, 22 S Greene St, Baltimore, MD N2W79A, USA

3 Department of Interventional Radiology, The University of Texas MD Anderson Cancer Center, Houston, TX, USA

4 Miami Cardiac and Vascular Institute, Miami, FL, USA

5 Division of Interventional Radiology, Department of Radiology, the University of Pennsylvania, Perelman School of Medicine, Philadelphia, PA, USA

6 Experimental Therapeutics Program, University of Maryland Marlene and Stewart Greenebaum Comprehensive Cancer Center, Baltimore, MD, USA

Mechanism

IRE involves the permeabilization of the cell membrane through the application of a high-voltage, low-energy direct current (DC), also referred to as a pulsed electric field (PEF) [1, 3]. The electric field generated between electrodes placed within or immediately adjacent to the tumor tissue induces a rapid buildup of electric charge across the plasma membrane (Fig. 1). When the transmembrane potential (TMP) reaches a critical threshold voltage, nanometer-sized pores start to form in the cell membranes and cause loss of homeostasis, followed by apoptosis and cell death [4, 5].

The extent of thermal damage is negligible in IRE compared to other thermal ablation methods, due to the unique energy delivery characteristics of IRE. Although some localized element of heat production adjacent to the electrodes (electrical Joule heating phenomenon) may still occur, the risk of this is minimal due to the short duration of the pulses, the low repetition rate of the pulses, and the extremely brief treatment time. Thus, tissue structures adjacent to the targeted lesion are preserved, including protein-rich extracellular matrix (ECM) and other sensitive structures that compose blood vessels and nerves [2, 6]. IRE also induces vascular congestion, which likely causes tissue hypoxia and may further accelerate tumor cell death [7].

During the procedure, IRE electrical pulses are synchronized with the cardiac R-waves [3]. Therefore, ECG monitoring is required for cardiac gating throughout the entire procedure, in addition to continuous monitoring of vital signs [8]. Cardiac stimulation devices or cardiac arrhythmias are the most important contraindications to IRE. Other relative contraindications include uncontrolled hypertension, epilepsy, and heart failure [9]. Metallic foreign objects, such as a pre-existing stent, in the ablation zone are not contraindicated. Although special attention should be paid to accurate positioning of the electrodes in patients with indwelling metallic stents in the biliary tree, the risk of short circuit if two activated electrodes are in contact with the metal can be easily minimized with the use of imaging to aid in clear visualization of the metallic stents [8]. Severe stenosis of the vasculature in or near the ablation zone and irreversible bleeding disorders are also considered relative contraindications.

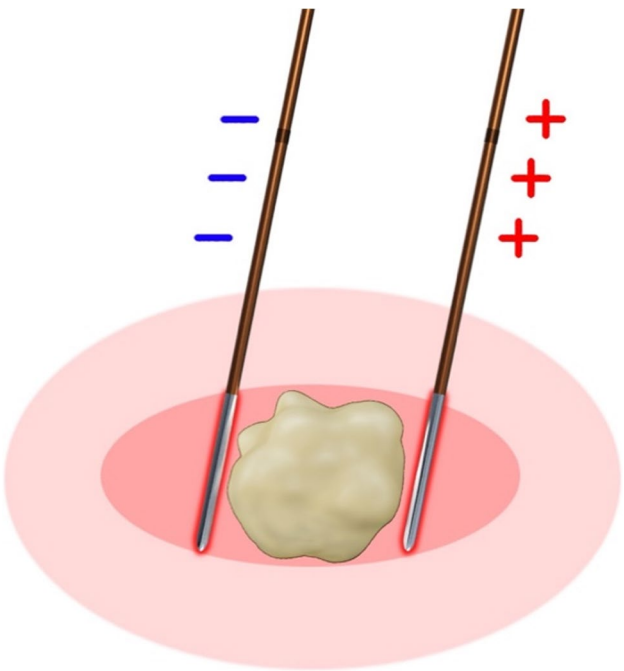

Fig. 1 Schematic illustration of IRE's mechanism of action

Image Guidance

The exact size and site of the target tumor are determined with one or more imaging modalities, such as computed tomography (CT), positron emission tomography (PET), and magnetic resonance imaging (MRI). IRE may be performed using contrast-enhanced ultrasound (CEUS) or either conventional or cone-beam CT. CEUS allows for continuous real-time observation of lesion tissue enhancement and can dynamically assess blood flow and tissue perfusion [5]. CT is the more commonly used modality due to its ability to create multiplanar reconstructions in real time. Patient position will likely differ between the prior imaging studies and the intraprocedural images while the patient is on the procedure table, so a CT scan should be performed during the procedure once anesthesia is initiated [8]. Additionally, rapidly growing tumors that have changed in size and appearance can be detected prior to the ablation if repeat intraprocedural imaging is performed.

Upon completion of the planned procedure, a final contrast-enhanced CT is performed to confirm complete coverage of the target and the ablation zone. IRE will form a sharp delineation between treated and unaffected areas in homogeneous tissue, usually with a peripheral zone of attenuation [6]. Gas is commonly visualized within post-IRE tumor tissue, due to dissociation of gas from the blood. This finding is a normal part of the electroporation process and is not due to gas-forming infection or bowel perforation [8].

Sedation

Unlike other ablation methods that allow for moderate sedation, all patients must undergo general anesthesia for IRE. To prevent skeletal muscle contractions stimulated by high-voltage electrical pulses and to minimize probe displacement, additional muscle relaxants are used for complete neuromuscular blockade [1, 3]. Supine and prone positions

are often preferred for IRE, as oblique positions are susceptible to patient slipping and repositioning [8]. The arms must also be carefully positioned to avoid brachial plexus injury. In case of ventricular arrhythmias during IRE, defibrillator pads can be placed prior to the procedure [3]. Antibiotic prophylaxis is recommended for all patients, and an indwelling Foley catheter is usually required until the patient has fully recovered from anesthesia. In cases of pancreatic or deep mesenteric lesions, bowel prep and oral contrast are usually administered to delineate adjacent bowel.

IRE Devices

Currently, the NanoKnife System (AngioDynamics, Queensbury, NY) is the only commercially available IRE treatment system and the only Food and Drug Administration (FDA)-approved system of IRE generators and electrodes for human tissue ablation (Fig. 2). This device has three components: the generator, probes, and AccuSync ECG device to prevent pulse-induced arrhythmias. In IRE, the area of ablation is roughly confined between the probes, compared to other ablation techniques in which the area of ablation radiates outward from the probes.

Two or more monopolar probes may be used to create a treatment zone. The number of electrodes used in the treatment is determined by the size of the tumor as with other ablation techniques; a maximum of six electrodes is allowed by the generator. For lesions smaller than 2 cm, three electrodes are placed at the periphery of the lesion; for lesions between 2-3 cm, four electrodes are placed at the periphery of the lesion; for lesions larger than 3 cm, four to six electrodes are used, with one to two electrodes placed at the center of the lesion [2].

When a pair of electrodes is used, the maximum distance between electrodes is 2.5 cm, with the optimal distance between the two electrodes being 0.7-2.9 cm [2, 8]. The probes must be inserted parallel to each other with a maximum angulation of 10° in order to avoid convergence or divergence of the probes, which will ensure uniform energy delivery and minimize nonuniform and heterogeneous ablation zones [1, 9]. A maximum of 2.5 cm is recommended for probe length, as longer electrodes result in higher current flow and increase the risk of high current cutoff [8]. If the target is larger than the exposed electrode length, the deepest portion of the target should always be treated first. The electrodes can be repositioned for each subsequent treatment to ensure adequate overlap at the junction of the two ablation zones.

When using multiple monopolar probes, the inter-electrode probe distance should be spaced between 1-2 cm, less than the maximum allowed inter-probe distance between an electrode pair, with a tumor-free margin of at least 5 mm. With three electrodes, the probes should be oriented around the lesion to form the vertices of a triangle; with four electrodes, the probes should be oriented around the lesion to form the vertices of a rectangle; with six electrodes, the probes should be oriented around the lesion to form the vertices of a hexagon. With multiple probes, multiple combinations of electrode pairs can be formed for each electrode, with the electrical pulses being fired between each pair and sequentially firing in a circumferential manner to cause multiple instances of electroporation within the tumor. Given

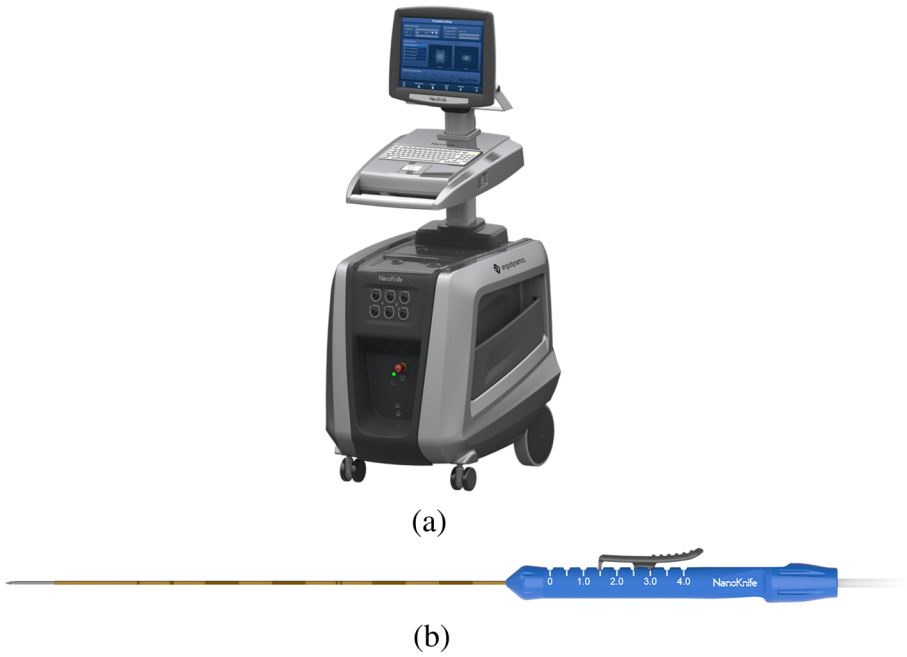

Fig. 2 AngioDynamics NanoKnife System **(a)** generator and **(b)** probe. Reprinted with permission. (https://www.angiodynamics.com/product/nanoknife-system/#productliterature)

that the procedure greatly relies on optimal probe placement for successful treatment of solid tumors, with precise placement of the bipolar probes at the same depth and in parallel, or multiple monopolar probes that are positioned exactly equidistant from each other and from the center of the tumor, the major intra-procedural outcome affected by the number of probes is the duration and technical success in treating the tumor. Additionally, greater probe counts allow for more room for error, because electrodes that are closer to each other than the desired distance will lead to overcurrent with unwanted joule heating, and electrodes that are farther from each other than the desired distance will lead to incomplete ablation.

The generator automatically displays a 2-dimensional (2D) representation of the tumor and the selected number of electrodes. In the case of a pair of electrodes, the interventionalist first enters the distance between electrodes of a pair and selects the desired voltage per centimeter (V/cm), usually 1200V/cm to 1800V/cm. Then, the generator delivers low-voltage, high-energy DC power through the tips of the electrode probes through a series of microsecond (μs) pulses at a repetition rate of one pulse per second [6, 8]. The electrical pulses should be delivered with voltages (V) ranging from 1,500 to 3,000V, as voltages less than 1,000V actually lead to reversible electroporation [2, 5]. Pulse length should always be set to 70-90 μs, and exposure length should be set at 20 mm [1, 5].

The generator can provide a maximum current of 50A [2], with targeted increase in current from 18-20A at baseline to 35–40A during IRE [8]. If the current does not sufficiently increase from baseline, the current can be increased by delivering additional pulses or increasing the exposure length. However, the latter is associated with a risk of ablating normal surrounding tissue. Persistently excessive current from the electrode(s) requires repositioning or removal of an electrode or pair of electrodes. In order to minimize this risk, AngioDynamics recommends an initial series check of 20 pulses per electrode to ensure that the current generated would not be excessive.

Treatment of Tumors

IRE allows for the ablation of tumors near heat-sensitive structures, especially nerves, blood vessels, and biliary ducts within the liver due to the sparing of connective tissue architecture [4]. Tumor tissue within the ablation zone is usually completely destroyed and necrotic, and interestingly, the ablation zone extends directly up to the vessel wall without sparing any tissue adjacent to the vessel but does not actually destruct or occlude the vessel itself [8, 10]. Due to higher performing costs compared to thermal ablation techniques, IRE is generally reserved for specific cases requiring these benefits to treat tumors near heat-sensitive structures. For instance, this procedure could decrease the incidence of biliary complications associated with hepatic tumor ablations, vascular and intestinal damage in pancreatic tumor ablations, collecting system damage in renal ablations, or urethral and rectal nerve damage in prostate ablations.

The most common tumors that are ablated using IRE are located in the liver, pancreas, kidney, and prostate. In fact, some consider IRE to be the first choice for ablation of any solid organ tumor except lung and bone tumors [8]. Similar to other ablation techniques, the best results are achieved with lesions under 3 cm in diameter, although meticulous positioning of the electrode probes could potentially allow for ablation of larger lesions, particularly within the liver and kidney. Complete ablation at the first attempt is less likely to occur for lesions larger than 3-4 cm in diameter. As the lesion volume increases, the time required to perform the required number of pulses results in a practical tumor size limit of 6-8 cm in maximum diameter [8]. Tumor recurrence is a potential risk associated with incomplete ablation in larger and heterogeneous tumors.

Liver Tumors

Hepatic tumors are among the most common tumors treated by interventional radiologists, and liver cancer is the second most common cause of cancer-related death worldwide [11]. RFA and MWA have been the standard of treatment for many malignant hepatic tumors, mainly HCC, colorectal liver metastases, and cholangiocarcinoma. IRE should be reserved for special circumstances and should only be considered if tumors are <5 cm and <1 cm away from the main bile ducts, intestinal structures, or vasculature [1].

Hepatocellular Carcinoma

Hepatocellular carcinoma (HCC) is responsible for 80% of the primary hepatic cancers [11], and several ablation options currently exist to treat these tumors. One study analyzed the differences in outcomes between MWA and IRE for patients diagnosed with Child-Pugh B HCC whose tumors were unresectable or treated as a bridge to transplantation [12]. Patients who underwent IRE had shorter post-ablation hospital stays, with an average of one day for IRE patients compared to two days for MWA patients [12]. Only four IRE patients were readmitted for procedure-related issues within 90 days of treatment compared to nine MWA patients, and the most common reasons for readmission included transient liver failure, dehydration, and uncontrolled ascites. Uncontrolled ascites was more severe in MWA patients compared to IRE patients. All of these differences were statistically significant with $P \leq 0.05$ [12]. Similar to this study, many other studies have demonstrated

that IRE is safe and effective in treating patients with HCC and underlying hepatic dysfunction. Patients who return to IR clinic for post-ablation care usually demonstrate successful treatment of the tumor with no residual enhancement at three months (Fig. 3).

Colorectal Liver Metastases

When surgical resection or thermal ablation are not feasible options, IRE should be considered, and the COLDFIRE-1 trial successfully demonstrated that IRE can completely eradicate vital colorectal metastatic tumor tissue [13]. A review of 12 studies involving 295 cases demonstrated efficacy rates of IRE therapy ranging from 74 to 100% with an average recurrence rate higher than 20% [2]. Severe complications are extremely rare, and more common adverse events include fever, pain, infection, abdominal ascites, nausea, vomiting, bleeding, gastric ulceration, liver abscesses, and myocardial infarction [2, 14]. Lesions close to the diaphragm are prone to irritation, and electroporation of local structures could potentially lead to significant pneumothorax and severe shoulder tip pain for several weeks [8].

Cholangiocarcinoma

Perihilar cholangiocarcinoma (PHC) is associated with poor outcomes, and only 20% of patients are candidates for curative surgery [15]. Almost half of all PHC patients already have metastatic disease at the time of diagnosis without substantial treatment options. Due to the nature of the tumor located at the hilum of the liver in close proximity to heat-sensitive structures, IRE is an appealing consideration in these patients. Franken et al. demonstrated that IRE combined with chemotherapy could be a favorable option for patients with PHC. The authors found no incidence of 90-day mortality in the study population and concluded a 5-month survival benefit of adding IRE to the standard of care treatment (21 versus 16 months for survival after diagnosis) [15]. Major adverse events are rare and can include pseudoaneurysm of the hepatic artery, recurrent bleeding, portal vein stenosis, or recurrent cholangitis.

Pancreatic Ductal Adenocarcinoma

Pancreatic ductal adenocarcinoma (PDAC) is one of the most aggressive pancreatic cancers. The 5-year survival rate is below 9%, and one-third of cases are non-metastatic locally advanced pancreatic cancer (LAPC) [9, 16]. These tumors can encase the superior mesenteric artery, celiac axis or portomesenteric veins, and consequently exclude surgical resection as a viable treatment option. Chemotherapy with or without radiation has traditionally been the first-line therapy for these tumors. However, many patients respond poorly to the current therapies due to the fibrotic and immunosuppressive tumor microenvironment of PDAC [14]. IRE has been shown to be a successful treatment modality with lower morbidity (24% vs 36%) and mortality (0% vs 2%) compared to surgery [13]. A literature review of 13 studies involving 391

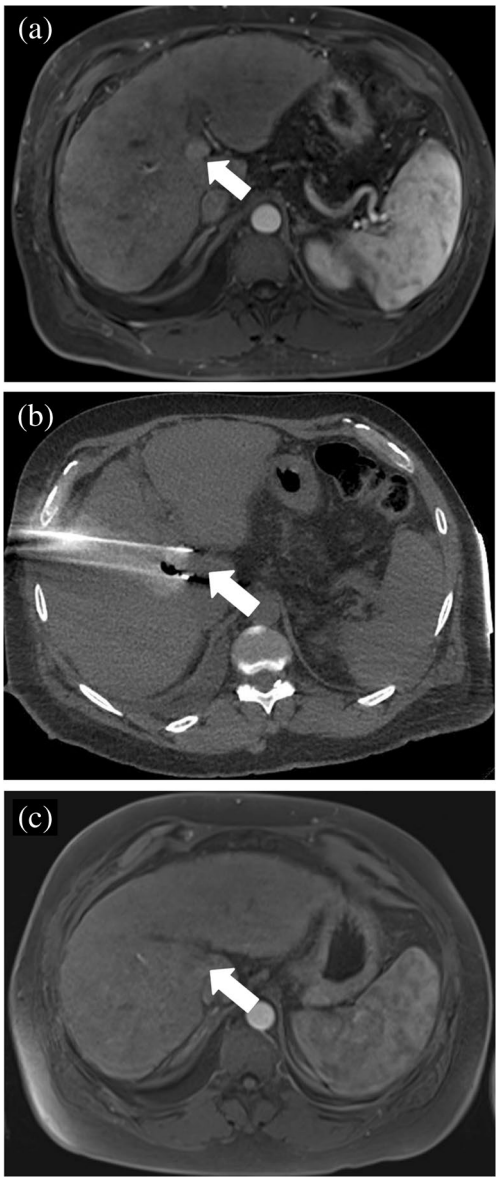

Fig. 3 A 49-year-old male with cirrhosis secondary to alcohol use complicated by portal hypertension. MRI of the abdomen with intravenous contrast showed a 2 cm LI-RADS 5 lesion in segment 4 near the hepatic hilum abutting the left and main portal veins. The patient underwent liver-directed IRE after a multidisciplinary tumor board discussion (a) pre-procedural MRI imaging demonstrates an enhancing mass (arrow) near the hepatic hilum. (b) intraprocedural CT imaging demonstrates two parallel probes with an enhancing zone of ablation in between the probes. Gas within the lesion (arrow) is an expected finding due to the dissociation of gases from the blood. (c) post-ablation 3-month follow-up MRI reveals hypoattenuation and lack of enhancement of the ablation target (arrow)

patients showed the effectivity rate of IRE to be 80–100% in some studies [2]. Minor adverse events caused by IRE in the pancreas are predominantly GI-related, such as abdominal pain, diarrhea, nausea, vomiting, loss of appetite, and delayed gastric emptying. Severe adverse events are uncommon and include vessel occlusion, bleeding, severe pancreatitis, and death. Preventative measures can be performed prior to the procedure to protect the stomach and duodenum by passing a nasojejunal feeding tube. Patients should be administered an oral proton pump inhibitor for 24–48 h after the procedure and advanced to standard oral feeding as tolerated [8]. A customized nutrition program may be tailored to each patient for better outcomes.

Renal Cell Carcinoma

Renal cell carcinoma (RCC) is the second most common malignant urinary tract neoplasm [15]. Traditional ablation options include RFA and MWA as thermal treatment modalities with cryoablation as an additional option. With the development of IRE, even tumors that were traditionally present in an unfavorable anatomic location, centrally located and close to the renal pelvis or the hilar vessels, are able to be treated with overall positive results without any severe complications. Because tumor size is a limiting factor when ablation is performed with curative intent, clinical T1a cancers are best suited for CT-guided IRE

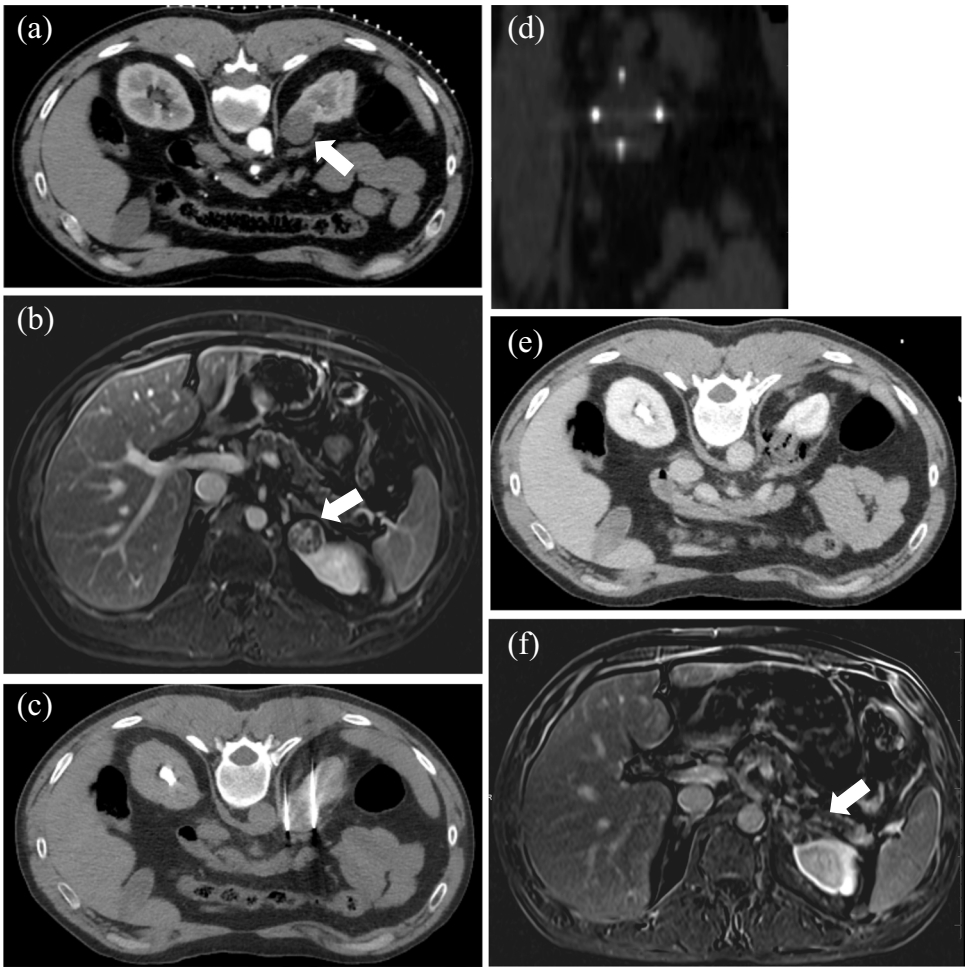

Fig. 4 A 48-year-old male, nonsmoker, with nephrolithiasis but otherwise no significant medical history with an incidental left renal mass (**a**) initial post-contrast axial CT demonstrates a hypoenhancing 3.0 cm × 2.6 cm exophytic lesion in the upper pole of the left kidney (arrow). (**b**) initial axial contrast-enhanced MRI confirms the presence of a complex cystic, exophytic, heterogeneously enhancing mass arising from the anterior upper pole of the left kidney (arrow), consistent with RCC. (**c**) axial CT slices demonstrate placement of two 17-Gauge 15 cm IRE probes during the procedure with (**d**) 3-dimensional (3D) reformatting of four probes in diamond-shaped configuration confirming the distance between the probes. (**e**) immediate post-ablation axial CT slice demonstrates an adequate ablation zone with expected gas visualized within and adjacent to the tumor tissues (**f**) the 18-month follow-up axial contrast-enhanced MRI demonstrates interval decrease in the size of the ablated lesion (arrow), measuring 1.5 cm × 1.4 cm without residual or recurrent enhancement (Images courtesy of Govindarajan Narayanan, MD, Miami Cancer Institute, Miami, FL)

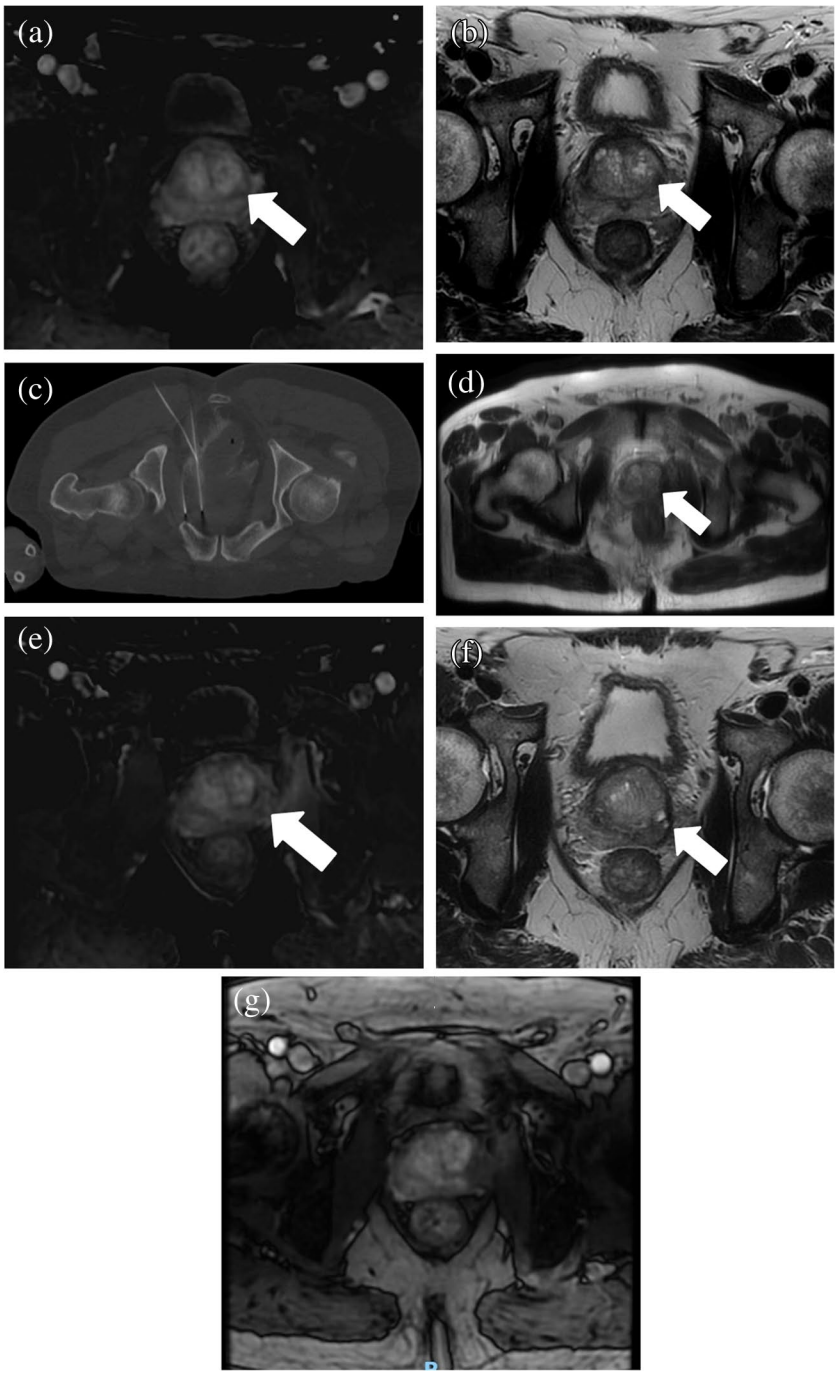

Fig. 5 A 68-year-old male with a lesion in the left postero-lateral peripheral zone at the mid prostate gland. Prostate-specific antigen (PSA) level was 9.0 ng/mL. Biopsy results confirmed adenocarcinoma in the left lateral and mid prostate gland with a Gleason score of 7, along with atypia in the left apex, base, right lateral prostate gland, and high-grade prostatic intraepithelial neoplasia. The patient underwent successful CT-guided IRE. (**a**, **b**) MRI images demonstrate cancer within the prostate gland (arrow). (**c**) intraprocedural CT image demonstrates IRE with hydrodissection. (**d**, **e**) post-ablation 3-month follow-up MRI demonstrates decreased enhancement within the target area. Post-ablation 9-month follow-up MRI with T2 (**f**) and dynamic contrast enhancement (**g**) images confirm lack of residual contrast enhancement

[17]. Clinical T1a RCC corresponds to small renal masses measuring ≤ 4 cm in the greatest dimension (Fig. 4). One retrospective study of 15 patients, including seven with solitary kidneys, saw a 100% procedural success rate [15]. Transient gross hematuria occurred in two patients, and the estimated glomerular filtration rate levels did not significantly change [15]. No recurrence was found at 6-month follow-up, and only one patient had needle tract metastasis at 1-year follow-up that required RFA therapy [15]. As a nephron-sparing ablation option, complete ablation had been achieved in all lesions at the time of the initial procedure, while the normal renal parenchymal vascular structure was well preserved [18]. Without the need for preoperative preparation such as pyelostomy, ureteral stent

implantation, and artificial pneumoperitoneum and ascites, IRE has become an even more favorable option for those who are eligible. While partial nephrectomy, cryoablation, and RFA are the primary approaches for the treatment of solitary renal solid lesions in suitable candidates, with long-term outcomes ranging from >97%, 86–94%, and 93–96%, respectively, compared to 91% in IRE [17], IRE has been associated with favorable outcomes, protecting renal function and allowing for ablations in anatomically high-risk RCC lesions.

Prostate Adenocarcinoma

Conventional therapy for localized prostate cancer often targets the whole prostate gland, which can lead to unfavorable side effects including incontinence, bowel dysfunction, and sexual dysfunction. Novel developments in prostate cancer treatment have focused on treating the cancerous portions of the prostate gland in order to spare normal prostate tissue. Prostate brachytherapy seeds are unlikely to interact with electrodes during IRE [8], which can be performed safely in the prostate gland (Fig. 5). One study showed that the 6-month clinically significant prostate cancer rate following IRE was only 1%, and patients' excellent functional outcomes in sexual and urinary questionnaires suggest minimal impact on quality of life [19].

Post-ablation Care

Patients are admitted for overnight observation. The median hospital stay is usually 3–4 days [9]. Pain control can be achieved with acetaminophen combined with an anti-inflammatory drug, although patient-controlled analgesia may be necessary for patients experiencing more severe pain. Post-ablation imaging is often obtained within 24–48 h to ensure complete ablation of the target tissue. Additionally, hematocrit level and chemistry panel should be evaluated prior to discharge. Consider antibiotic and thrombotic prophylaxis for the duration of the hospital stay until discharge.

A CT or MRI with intravenous contrast is recommended at one month following the procedure. The zone of peripheral contrast enhancement is commonly no longer present at one month, and any enhancement previously seen within the target zone should have resolved. On the other hand, PET is often performed more than 3 months after the procedure, as PET images may show a photopenic region at the site of ablation with variable activity at the margins of the ablation zone similar to the zone of enhancement [8].

Fig. 6 Schematic picture of H-FIRE probe tip

Challenges

1. Minimum of two probes are required due to unipolarity of probes.
2. The needles must be placed parallel to each other within 2 cm, as any angle could result in arching phenomena.
3. Requires general anesthesia with muscle relaxant.
4. Requires cardiac synchronization.

New Developments

High-Frequency IRE (H-FIRE)

Traditional IRE pulses have been unipolar with a strong DC frequency component (0 Hz) [6]. The first-generation IRE is limited by muscle contraction and electrode movement due to electric field sinks caused by adjacent large blood vessels [20]. Muscle contractions can affect electrode positioning, invalidate treatment planning algorithms, and harm surrounding vital structures.

H-FIRE is a novel technique that involves the use of high-frequency, bipolar bursts (Fig. 6). Square-wave bursts with a center frequency around 500 kHz produce more

homogeneous, predictable electric field distributions. As the frequency of the applied electric field increases, the electrical impedance decreases and reduces the potential for thermal damage. These bursts can overcome the impedance barrier of the skin or other epithelial layers, which normally are more susceptible to thermal damage from sublethal electric fields and low conductivity of the skin [6]. In addition, muscle contractions can be eliminated during H-FIRE.

The critical threshold TMP across the plasma membrane is 1V for IRE. A study performed using rat brain tissue demonstrated that H-FIRE with bipolar bursts at frequencies of 250 kHz and 500 kHz can maintain the potential to overcome impedance barriers posed by epithelial layers. The increased center frequency of bipolar waveforms increases the threshold for nerve stimulation [6]. The study also confirmed the non-thermal effect of cell death in IRE and demonstrated that the application of 180 bursts with a pulse on-time of 200 µs causes only a 3.5°C increase in temperature near the electrode boundaries. This results in a 0.3% probability of cell death from thermal processes [6]. Compared to traditional IRE pulsing protocols associated with macroscopic muscular contractions, H-FIRE protocols eliminate all visual or tactile evidence of muscular contraction above the inherent noise of the system, even at the highest energy bursts. The study suggests that the clinical application of IRE without the administration of paralytic agents is possible with H-FIRE using up to 1 MHz for an electric field of 1,500V/cm.

Another study by Wang et al. revealed H-FIRE results from a phase 1 clinical trial performed at four medical centers on human participants with prostate cancer. The primary outcome included clinically significant PCa (csPCa), which was defined as any biopsy core with a Gleason score of ≥7, Gleason score of 6 plus maximum cancer core length > 3 mm, or an increase from the original cancer burden. Other clinical assessments evaluated were the International Prostate Symptom Score (IPSS), International Index of Erectile Function (IIEF-5), and diaper usage. There were no intraoperative complications seen with H-FIRE. In 100 patients who underwent H-FIRE, the 6-month biopsy results revealed six csPCa (one in the treatment zone and five outside the treatment zone), which corresponds to a lower rate of csPCa (6%) versus the historical control (20%) [19]. A total of 41 complications occurred in 29 patients (overall complication rate of 37.6%) during the follow-up time frame [20]. The most common complications were pyuria, epididymitis, gross hematuria, urinary retention, urinary tract infection, and bladder calculi. Significant reduction in tumor size was not associated with significant changes in the IPSS or IIEF-5 scores. Overall, this study supports the safety and efficacy of treating prostate cancer with H-FIRE.

Probes with Different Voltage

Compared to reversible electroporation, IRE requires more pulses (at least 80–100 pulses) and a higher amplitude (up to 3,000V) [21]. Electrical pulses usually include eight square-wave pulses of 100 µs, with an amplitude of 100V to 1,000V. A prior study evaluating H-FIRE at center frequencies of 0, 100, 250, 500, and 1,000 kHz reported that at 250 kHz, IRE is possible during all waveforms [6]. However, at 500 kHz, only the waveforms with amplitudes of 1,500V/cm are capable of inducing IRE. At 1 MHz, only the 1,500V/cm waveform with delays can cause IRE [6].

An Alternative PEF System: Aliya™ System

The Aliya™ System (Galvanize Therapeutics, GTI-00018 investigational device, San Carlos, CA) (Fig. 7) is a newly FDA-cleared PEF ablation system intended for ablation of

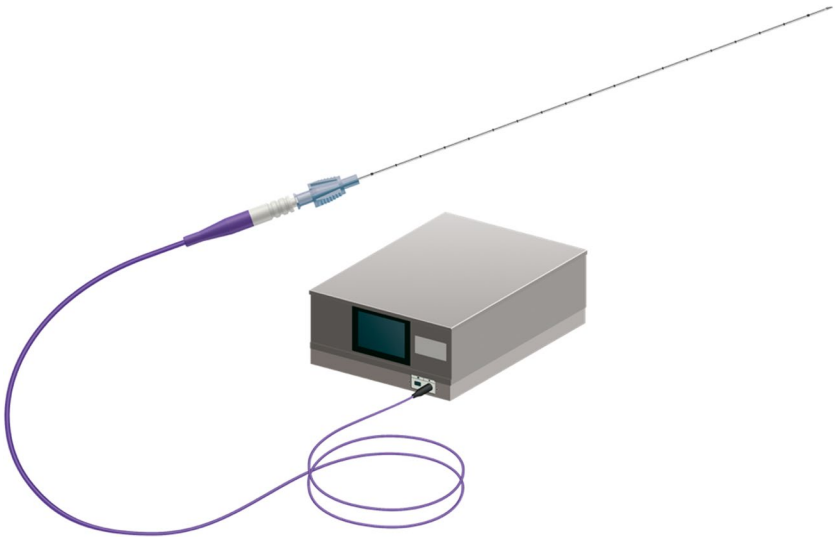

Fig. 7 Schematic Image of the Aliya™ System by Galvanize Therapeutics. Reprinted with permission

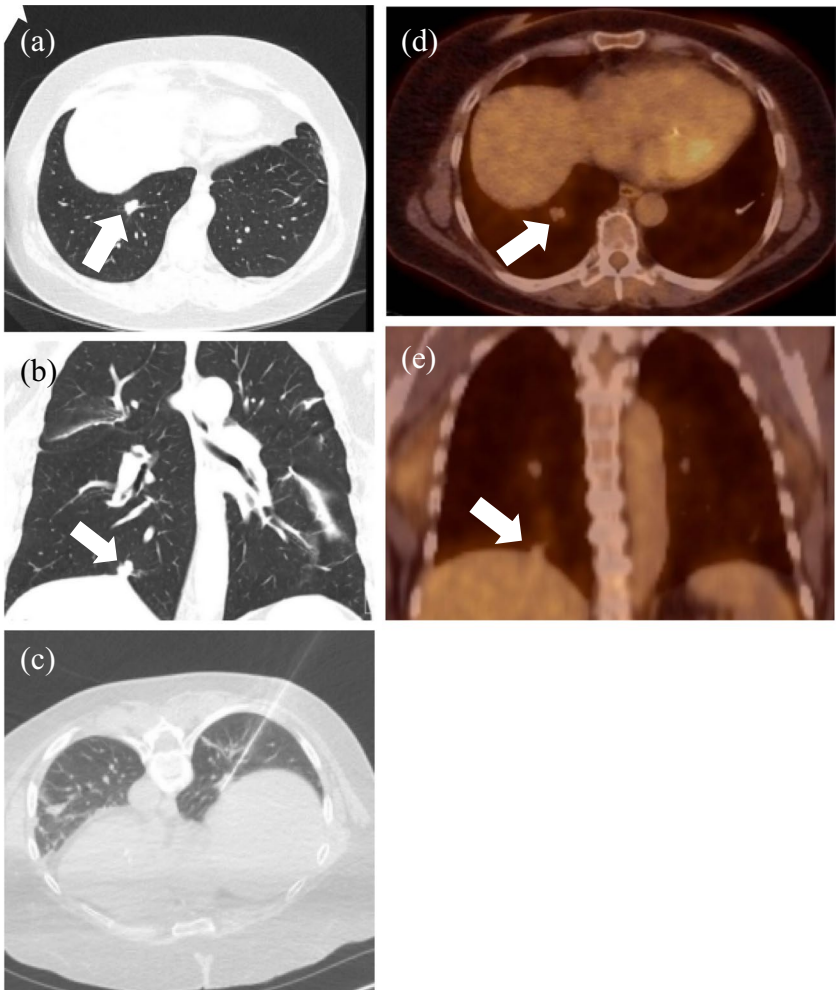

Fig. 8 A 43-year-old female with a past medical history of metastatic CRC status post partial lobectomy x2 (2018) and recurrence at the right lung base status post cryoablation (2020), returned 20 months later for management of a recurrent 1.6 cm nodule (2022). Axial (**a**) and coronal (**b**) unenhanced CT images demonstrate a single nodule (arrow) at the right lung base. (**c**) The patient was treated with the Aliya System in three overlapping 5-minute ablation zones using a single probe. No diaphragmatic injury occurred during the procedure. Post-ablation PET axial (**d**) and coronal (**e**) images demonstrate stable size of the nodule (arrow) and no FDG activity at 6-month post ablation follow-up

soft tissues, including liver and lung, that achieves its results via a slightly different PEF mechanism than IRE. This system requires only a single monopolar 19-gauge 20 cm needle, rather than multiple monopolar or bipolar electrodes as in IRE, to deliver non-thermal PEF to disrupt cellular homeostasis and cause apoptosis [22]. The Aliya System releases PEF through pulse trains consisting of biphasic waveforms lasting mere nanoseconds, while the traditional IRE application releases PEF through single pulses consisting of monophasic waveforms lasting hundreds of milliseconds. Because the PEF pulse train duration is extremely short, less than the duration of a QRS wave, PEF ablation does not interfere with the cardiac cycle and usually will not cause peripheral nerve stimulation, eliminating the need for pre-procedural administration of paralytics. As a result, the PEF system is designed for use near critical structures, as it also preserves the ECM, nerves, ducts, and vessels the way IRE does. Additionally, this system may be combined with other immunotherapies, as the treatment could result in antigen release that could activate the immune system. The major appeal of the Aliya System is the potential to

Fig. 9 A picture of IMACTIS-CT navigation system (https://www.imactis.com/en/ct-navigation). Reprinted with permission

treat non-small cell lung cancer, a tumor that has not been a target of conventional IRE (Fig. 8). The Aliya System may be deployed either transbronchially or percutaneously, and initial INCITE-ES clinical trials conducted outside the USA have demonstrated early technical success in ablating non-small cell lung cancer [23].

Needle Placement Navigation Systems

Precise and accurate probe placement is critical for optimal tumor ablation. Several commercially available navigation systems exist to aid with percutaneous interventions. IMACTIS-CT (IMACTIS, Grenoble, France) (Fig. 9) provides stereotactic needle guidance to enable pre-planning and continuous control. The benefit of 3D live needle tracking with reproduction of the planned trajectory and continuous needle depth measurement is the significantly improved accuracy of needle placement resulting in decreased needle placement scans and radiation dose. CAS-One IR (CAScination AG, Bern, Switzerland) is another stereotactic navigation system that compares the planned path with the real-time needle trajectory and assists in the insertion of the ablation probe. While less commonly used, robot-assisted navigation systems have also been utilized in several institutions [4]. Maxio (Perfint Healthcare, Chennai, India) actively guides placement of the instruments by defining entry point, angle, and depth, although it does not track needle position in real time. The Maxio can automatically determine the order of electrode placement to avoid collision with the positioner and previously placed electrodes. A simple Faraday probe and oscilloscope connected to a computer can assess each delivered pulse. The Faraday probe can allow for early detection of overcurrent and can prevent the need for generator shutdown and cold restart [8]. A smaller navigation system called iSYS (iSYS Medizintechnik GmbH, Kitzbuehel, Austria) consists of a small device mounted to the CT table, which registers radiopaque markers on the robotic device to assist with image acquisition during pre-procedural planning.

Robotic Needle Placement

Due to the importance of precise needle placement in IRE, robotic assistance has emerged as a way to improve accuracy, safety, and efficiency of the procedure. More accurate needle placement will increase the possibility of successful tumor ablation, decrease procedure duration by decreasing the number of needle adjustments and angulations, and decrease radiation. One study showed that the time from the planning CT scan to the start of the ablation and the dose-length product were significantly lower under robotic assistance (63.5 vs. 87.4 min, $P<0.001$; 2132 vs. 4714 mGy-cm, $P<0.001$) [24]. The procedural accuracy, measured as the deviation of the IRE probes with respect to a defined reference probe, was significantly higher using robotic guidance (2.2 vs. 3.1 mm, $P<0.001$). There were no complications. There was one incomplete ablation in the manual group [24]. An example of a robotic device for IRE is the Epione® robotic device (Quantum Surgical, Montpellier, France), recently Conformite Europeenne (CE)-marked and FDA-cleared for all abdominal lesions, which assists the physician during CT-guided percutaneous needle insertion [27]. This device consists of a mobile

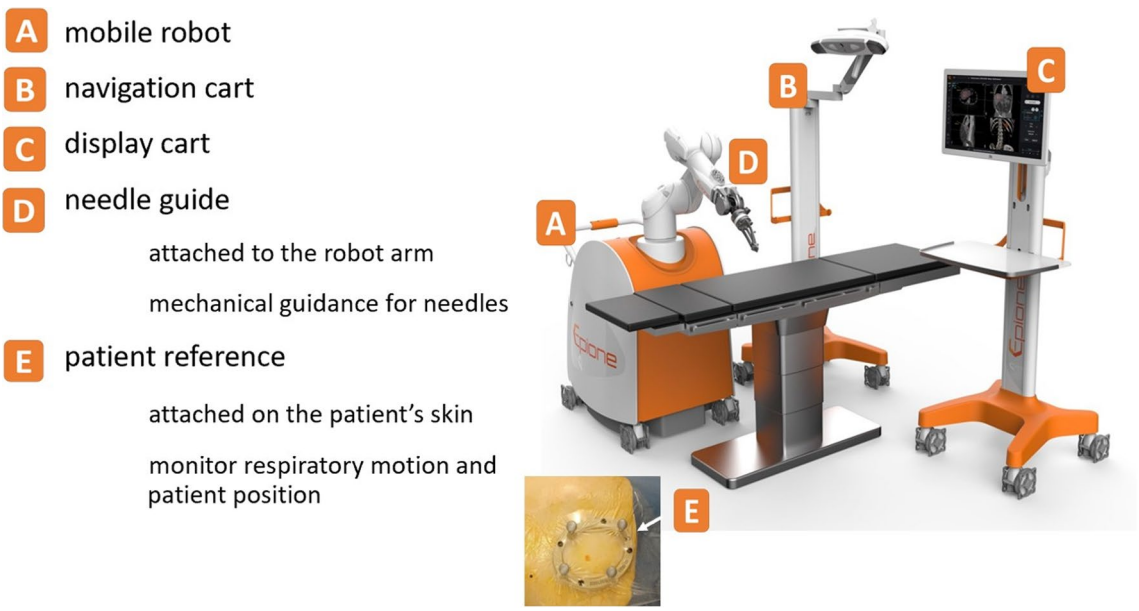

Fig. 10 The Epione® robotic platform from Quantum Surgical. Reprinted with permission

cart that carries a robotic arm bearing a needle guide, a mobile display cart, a patient reference attached to the skin that monitors patient motion and respiration, and a navigation camera (Fig. 10). Robotic assistance can be used from the start of the planning stage, where physicians can define the tumor and margin on a CT or MRI study, select the ablation modality and number of probes, and visualize the ablation zone coverage with 2D/3D image fusion software. Immediately prior to the procedure start, the robot is registered to the patient. Respiratory monitoring is used to synchronize CT acquisitions and robotically-assisted needle insertion, ensuring the target organ is repositioned accurately with each apnea induction. During the procedure, the robot guides the needle into the target down the planned trajectory in one push from skin to target and delivers the ablative therapy. Upon the completion of the procedure, the robotic system is able to acquire post-ablation CT images and overlay them with pre-procedure images and quantify minimal ablation margins to assess results. Initial trials were performed on swine kidney and liver models [25, 26], which demonstrated feasibility, safety and accuracy of the device in these two lesion locations. Accuracy was not impacted by the trajectory length or angulation. Feasibility and safety were confirmed in a bicentric prospective study that included 21 patients with HCC or liver metastases [28]. Robotic-assisted ablation was feasible in 95.7% of lesions, with no adverse events reported [28]. To date, three cancer centers have successfully treated around 200 patients with robotic assistance.

Immunomodulation and Combining IRE with Immunotherapies

Following ablation in tumor tissue, the body generates immune responses by increasing the availability of tumor-specific antigens. Recent studies have shown that IRE promotes the massive release of intracellular tumor antigens that become an "in situ tumor vaccine." The resulting effect aids in killing residual tumor cells and inhibiting local recurrent and distant metastasis following IRE [2].

An animal model study focusing on HCC showed that IRE can generate neoantigen-specific T cells by the following mechanisms: (i) increase the synthesis and secretion of damage-associated molecular patterns (DAMPs) from injured cells and induce immunogenic cell death, (ii) activate tumor antigen-specific T cells when dendritic cells in tumor tissues take up the DAMPs and migrate to draining lymph nodes, and (iii) expand the number of immunosuppressive T cells [2]. The release of DAMPs is stimulated by greater electric field strengths. As T cell infiltration and immune memory increases, cell death also increases. Reactive oxygen species (ROS)-dependent apoptosis has been shown to mediate inhibition of the PI3K-Akt pathway in pancreatic cancer [29]. Programmed death-ligand 1 (PD-L1) also has been shown to promote $CD8^+$ T cell dysfunction and inhibit PD-L1, slowing tumor growth in hepatic cancer. Multiple studies have reported a promising benefit of IRE as an immunomodulatory therapy in combination with immunotherapy [30].

A clinical study of prostate cancer demonstrated that IRE treatment-mediated T cell immune response occurred between 3 and 5 days after IRE ablation, which provides a window for maximizing treatment efficacy in combination with immunotherapy. Using immune checkpoint inhibitors (ICI), previous studies have demonstrated that blocking inhibitory proteins cytotoxic T-lymphocyte associated-protein 4 (CTLA-4) and programmed cell death protein-1 (PD-1) on exhausted $CD8^+$ T-cells results in tumor remission. Tumors treated with IRE and anti-CTLA-4 ICI promoted robust expansion of tumor-specific $CD8^+$ cells in blood, tumor, and non-lymphoid tissues (NLTs) [31]. IRE treatments combined with DC vaccination, PD-1 inhibitor, with or without Toll-like receptor-7 (TLR7) agonist, ICIs and immunostimulants, or allogenic natural killer cells, can prolong overall survival and improve immune status [2].

A triple therapy consisting of IRE, αPD-1 therapy, and a nanoformulation (dMSN-SB) has been shown to inhibit transforming growth factor β (TGF-β) signaling in pancreatic cancer through rapid infiltration of tumor-associated neutrophils (TANs) [16]. Due to the abundance of TANs in post-IRE tumors, TAN modulation enhances the combined antitumor efficacy of IRE and αPD-1 therapy to yield better outcomes.

Various combinations of the IRE procedure, immunomodulatory therapy, and immunotherapy have demonstrated safe, effective outcomes and can enhance treatment response compared to the IRE procedure alone.

Conclusion

IRE is a safe and effective treatment option for tumor ablation at the target site. Compared with other ablation techniques, IRE has several advantages, such as absence of the heat sink effect and minimal injury to blood vessels and bile ducts while activating the immune system. As a result, IRE can be repeated if necessary. Novel techniques such as H-FIRE, needle placement systems, and robotics have enhanced the accuracy and performance in placement of IRE probes. Prior studies have also shown that IRE can be especially beneficial when combined with chemotherapy, immunomodulation, and immunotherapy.

Acknowledgements The authors thank Dr. Govindarajan Narayanan, MD, from the Miami Cancer Institute for providing a case of the successful treatment of renal cell carcinoma through irreversible electroporation.

Declarations

Conflict of Interest The authors declare no competing interests.

Human and Animal Rights and Informed Consent This article does not contain any studies with human or animal subjects performed by any of the authors.

References

1. Ruarus AH, Vroomen LGPH, Puijk RS, Scheffer HJ, Zonderhuis BM, Kazemier G, van den Tol MP, Berger FH, Meijerink MR. Irreversible Electroporation in Hepatopancreaticobiliary Tumours. Can Assoc Radiol J. 2018;69(1):38–50. https://doi.org/10.1016/j.carj.2017.10.005.
2. Zhang N, Li Z, Han X, Zhu Z, Li Z, Zhao Y, Liu Z, Lv Y. Irreversible Electroporation: An Emerging Immunomodulatory Therapy on Solid Tumors. Front Immunol. 2022;12:811726. https://doi.org/10.3389/fimmu.2021.811726.
3. Narayanan G. Irreversible Electroporation. Semin Intervent Radiol. 2015;32(4):349–55. https://doi.org/10.1055/s-0035-1564706.
4. Fuhrmann I, Probst U, Wiggermann P, Beyer L. Navigation Systems for Treatment Planning and Execution of Percutaneous Irreversible Electroporation. Technol Cancer Res Treat. 2018;17:1533033818791792. https://doi.org/10.1177/1533033818791792.
5. Zhou L, Yin S, Chai W, Zhao Q, Tian G, Xu D, Jiang T. Irreversible electroporation in patients with liver tumours: treated-area patterns with contrast-enhanced ultrasound. World J Surg Oncol. 2020;18(1):305. https://doi.org/10.1186/s12957-020-02083-4.
6. Arena CB, Sano MB, Rossmeisl JH Jr, Caldwell JL, Garcia PA, Rylander MN, Davalos RV. High-frequency irreversible electroporation (H-FIRE) for non-thermal ablation without muscle contraction. Biomed Eng Online. 2011;10:102. https://doi.org/10.1186/1475-925X-10-102.
7. Al-Sakere B, André F, Bernat C, Connault E, Opolon P, Davalos RV, Rubinsky B, Mir LM. Tumor ablation with irreversible electroporation. PloS One. 2007;2(11):e1135. https://doi.org/10.1371/journal.pone.0001135.
8. Thomson KR, Kavnoudias H, Neal RE 2nd. Introduction to Irreversible Electroporation—Principles and Techniques. Tech Vasc Interv Radiol. 2015;18(3):128–34. https://doi.org/10.1053/j.tvir.2015.06.002.
9. Timmer FEF, Geboers B, Ruarus AH, Schouten EAC, Nieuwenhuizen S, Puijk RS, de Vries JJJ, Meijerink MR, Scheffer HJ. Irreversible Electroporation for Locally Advanced Pancreatic Cancer. Tech Vasc Interv Radiol. 2020;23(2):100675. https://doi.org/10.1016/j.tvir.2020.100675.
10. Rubinsky B, Onik G, Mikus P. Irreversible electroporation: a new ablation modality—clinical implications. Technol Cancer Res Treat. 2007;6(1):37–48. https://doi.org/10.1177/153303460700600106.
11. Zimmerman A, Grand D, Charpentier KP. Irreversible electroporation of hepatocellular carcinoma: patient selection and perspectives. J Hepatocell Carcinoma. 2017;4:49–58.
12. Bhutiani N, Philips P, Scoggins CR, McMasters KM, Potts MH, Martin RCG. Evaluation of tolerability and efficacy of irreversible electroporation (IRE) in treatment of Child-Pugh B (7/8) hepatocellular carcinoma (HCC). HPB. 2016;18(7):593–399. https://doi.org/10.1016/j.hpb.2016.03.609.
13. Scheffer HJ, Vroomen LG, Nielsen K, van Tilborg AA, Comans EF, van Kuijk C, van der Meijs BB, van den Bergh J, van den Tol PM, Meijerink MR. Colorectal liver metastatic disease: efficacy of irreversible electroporation—a single-arm phase II clinical trial (COLDFIRE-2 trial). BMC Cancer. 2015;15:772. https://doi.org/10.1186/s12885-015-1736-5.
14. Alnaggar M, Qaid AM, Chen J, Niu L, Xu K. Irreversible electroporation of malignant liver tumors: Effect on laboratory values. Oncol Lett. 2018;16(3):3881–8. https://doi.org/10.3892/ol.2018.9058.
15. Franken LC, van Veldhuisen E, Ruarus AH, Coelen RJS, Roos E, van Delden OM, Besselink MG, Klümpen HJ, van Lienden KP, van Gulik TM, Meijerink MR, Erdmann JI. Outcomes of Irreversible Electroporation for Perihilar Cholangiocarcinoma: A Prospective Pilot Study. J Vasc Interv Radiol. 2022;33(7):805-813.e1. https://doi.org/10.1016/j.jvir.2022.03.024.
16. Peng H, Shen J, Long X, Zhou X, Zhang J, Xu X, Huang T, Xu H, Sun S, Li C, Lei P, Wu H, Zhao J. Local Release of TGF-β Inhibitor Modulates Tumor-Associated Neutrophils and Enhances Pancreatic Cancer Response to Combined Irreversible Electroporation and Immunotherapy. Adv Sci (Weinh). 2022;9(10):e2105240. https://doi.org/10.1002/advs.202105240.
17. Wah TM, Lenton J, Smith J, Bassett P, Jagdev S, Ralph C, Vasudev N, Bhattarai S, Kimuli M, Cartledge J. Irreversible electroporation (IRE) in renal cell carcinoma (RCC): a mid-term clinical experience. Eur Radiol. 2021;31(10):7491–9. https://doi.org/10.1007/s00330-021-07846-5.
18. Wang Z, Lu J, Huang W, et al. A retrospective study of CT-guided percutaneous irreversible electroporation (IRE) ablation: clinical efficacy and safety. BMC Cancer. 2021;21:124. https://doi.org/10.1186/s12885-021-07820-w.
19. Ng H, Wang K, Cartledge J, et al. Ureteric Injury after Image-Guided Ablation of Renal Cell Cancer with Irreversible Electroporation. JVIR. 2020;32(2):P322-324. https://doi.org/10.1016/j.jvir.2020.09.015.
20. Wang H, Xue W, Yan W, et al. Extended Focal Ablation of Localized Prostate Cancer With High-Frequency Irreversible Electroporation: A Nonrandomized Controlled Trial. JAMA Surg. 2022;157(8):693–700. https://doi.org/10.1001/jamasurg.2022.2230.
21. Geboers B, Scheffer HJ, Graybill PM, Ruarus AH, Nieuwenhuizen S, Puijk RS, van den Tol PM, Davalos RV, Rubinsky B, de Gruijl TD, Miklavčič D, Meijerink MR. High-Voltage Electrical Pulses in Oncology: Irreversible Electroporation, Electrochemotherapy, Gene Electrotransfer, Electrofusion, and Electroimmunotherapy. Radiology. 2020;295(2):254–72. https://doi.org/10.1148/radiol.2020192190.
22. Galvanize Therapeutics, Inc. Aliya System. https://galvanizetx.com/aliya-system. Accessed 20 June 2023.
23. Endovascular Today. Galvanize Therapeutics' Aliya PEF System Studied in Solid Tumors. https://evtoday.com/news/galvanize-therapeutics-aliya-pef-system-studied-in-solid-tumors. Accessed 20 June 2023.
24. Beyer LP, Pregler B, Michalik K, Niessen C, Dollinger M, Müller M, Schlitt HJ, Stroszczynski C, Wiggermann P. Evaluation of a robotic system for irreversible electroporation (IRE) of malignant liver tumors: initial results. Int J Comput Assist Radiol Surg. 2017;12(5):803–9. https://doi.org/10.1007/s11548-016-1485-1.
25. de Baere T, Roux C, Noel G, Delpla A, Deschamps F, Varin E, Tselikas L. Robotic assistance for percutaneous needle insertion in the kidney: preclinical proof on a swine animal model. Eur Radiol Exp. 2022;6(1):13. https://doi.org/10.1186/s41747-022-00265-1.
26. Guiu B, De Baère T, Noel G, et al. Feasibility, safety and accuracy of a CT-guided robotic assistance for percutaneous needle

placement in a swine liver model. Sci Rep. 2021;11:5218. https://doi.org/10.1038/s41598-021-84878-3.
27. Epione. Quantum Surgical. https://www.quantumsurgical.com/epione/ [Accessed 25 June 2023].
28. de Baère T, Roux C, Deschamps F, Tselikas L, Guiu B. Evaluation of a New CT-Guided Robotic System for Percutaneous Needle Insertion for Thermal Ablation of Liver Tumors: A Prospective Pilot Study. Cardiovasc Intervent Radiol. 2022;45(11):1701–9. https://doi.org/10.1007/s00270-022-03267-z.
29. Sun S, Liu Y, He C, Hu W, Liu W, Huang X, et al. Combining NanoKnife With M1 Oncolytic Virus Enhances Anticancer Activity in Pancreatic Cancer. Cancer Lett. 2021;502:9–24. https://doi.org/10.1016/j.canlet.2020.12.018.
30. Qian J, Chen T, Wu Q, Zhou L, Zhou W, Wu L, et al. Blocking Exposed PD-L1 Elicited by Nanosecond Pulsed Electric Field Reverses Dysfunction of CD8 T Cells in Liver Cancer. Cancer Lett. 2020;495:1–11. https://doi.org/10.1016/j.canlet.2020.09.015.
31. Burbach BJ, O'Flanagan SD, Shao Q, Young KM, Slaughter JR, Rollins MR, Street TJL, Granger VE, Beura LK, Azarin SM, Ramadhyani S, Forsyth BR, Bischof JC, Shimizu Y. Irreversible electroporation augments checkpoint immunotherapy in prostate cancer and promotes tumor antigen-specific tissue-resident memory CD8+ T cells. Nat Commun. 2021;12(1):3862. https://doi.org/10.1038/s41467-021-24132-6.